



Universiteit
Leiden
The Netherlands

Design, synthesis, characterization and biological studies of ruthenium and gold compounds with anticancer properties

Garza-Ortiz, A.

Citation

Garza-Ortiz, A. (2008, November 25). *Design, synthesis, characterization and biological studies of ruthenium and gold compounds with anticancer properties*. Retrieved from <https://hdl.handle.net/1887/13280>

Version: Corrected Publisher's Version

License: [Licence agreement concerning inclusion of doctoral thesis in the Institutional Repository of the University of Leiden](#)

Downloaded from: <https://hdl.handle.net/1887/13280>

Note: To cite this publication please use the final published version (if applicable).

CHAPTER 2

Novel Mononuclear Gold(III) Complexes with Modified 2-(arylamino)pyridine Ligands: Synthesis and Characterization*

Abstract

Gold drugs were introduced into clinical applications from the mid 20th century; they are mainly administered for the treatment of rheumatoid arthritis and classified in the disease-modifying antirheumatic drugs (DMARD) class. After the introduction of auranofin in 1985 no new gold-based drugs have been clinically approved. Despite the apparent lack of interest in new gold-based therapeutics for rheumatic diseases, enormous attention has been directed in the use of gold compounds for cancer therapy.

Owing to the close similarities (structure and electronic configuration) of Gold(III) and platinum(II) complexes, d⁸ square-planar gold(III) compounds are of potential interest as anticancer agents, mainly because it is tempting to speculate that such complexes would have similar antitumor activity as cisplatin.

The chemistry and biological activity of gold(III) complexes have been scarcely investigated primarily because of their relatively high reactivity. Gold(I) compounds possess much better stability tendencies and this is partially the reason of major interest in gold(I) research. In order to accomplish sufficient chemical stability, towards reduction of the metal, the appropriate choice of the ligand coordinated to the gold(III) centre is a key factor.

In this chapter the synthesis and characterization of novel Au(III) complexes, with modified 2-(arylamino)pyridine ligands are described in detail. The ligands selected for this study are derivatized arylazopyridines, with electron-donating groups, either in the pyridyl moiety, the aryl one or both. The complexes are also designed with two monodentate chloride ligands which could be hydrolyzed and make 2 sites available for substitution.

The novel Au(III) compounds were characterized by means of elemental analysis, IR, UV-Vis, conductivity measurements, ¹H NMR, ESI-MS and ICP-OES. This work intends to address a variety of closely related ligands in order to determine the complex-stability tendency, which could help in further understanding and establishment of the proper structure-activity relationships.

"It owes its perfection to the unique and admirable balance of elementary constituents and virtues therein. In addition, it harbours specific virtues which are due to celestial influence. In its stability and permanence, gold is itself like a star of heaven.

Though an object composed of elements, it is unalterable, insoluble, incorruptible, a miracle of nature. It helps vision, and above all, cleanses and clears the substances of the heart and the fountain of life"

Arnald of Villanova (1235-1311)[1]

"I am among those who think that science has great beauty. A scientist in his laboratory is not only a technician: he is also a child placed before natural phenomena which impress him like a fairy tale"

Marie Curie, scientist (1897-1956)

* The results presented in this chapter have been published in Garza-Ortiz, A.; den Dulk, H.; Brouwer, J.; Kooijman, H.; Spek, A. L. and Reedijk, J., J. Inorg. Biochem.101 (2007) 1922.

2.1. Introduction

Clearly, the use of metal ions in medicine is not a new trend. It is well known that many metal ions are essential nutrients, and also that many are becoming increasingly widespread components of diagnostic or therapeutics for studying or treating a wide variety of diseases and metabolic disorders.

Despite the historical method of drug discovery, based on trial-and-error testing of chemical substances, the ongoing trend is the purposeful design of metal-based therapeutics. There are several reasons to stimulate the design of metal-base therapeutics in a more efficient way, which include, not only reduction of side effects in previously discovered drugs, improvements in the efficacy, adjustment of best pattern of administration and doses, selection of best route of medication, or the best combined treatment, but also, and not less important, the potential reduction in costs. Nowadays, the design of metal-based compounds with well-defined absorption, distribution, metabolism and excretion mechanisms is an urgent need.

The challenge is enormous considering the complexity of the drug-design process itself. Further challenges in the field, are the development of efficient predictive methods for metal-based compounds of therapeutic interest, improvements in the methods for detection of biological activity and even improvements in the standard procedures for the selection of the most efficient drug for a particular illness.

When talking about metal-based drug design, choices are not easy to be taken. Varying the ligand coordinated to the metal, for instance, is one obviously verifiable way of altering the endogenous distribution of metal ions in the body; however, not specific guidelines are available to predict the effects of variations *a priori*. Tissue targeting is a highly desirable goal for metal-based therapeutics or diagnostics, but it is not always feasible and more specific targeting ligands must be found. Not only the right ligand, but also the right metal-ligand combination, is important. In a metal-containing compound, the ligand is often, but not always, an organic compound that binds metal ions and modifies the physical and chemical properties of them. In biological systems metal ions promote responses that range from deficiency to toxicity. In addition, whether essential or not, the threshold for toxicity can be very low. For example, platinum, although not an essential element, is a critically important therapeutic agent in cancer therapy, despite its well-known toxic potential.

The design and testing of gold complexes as antitumour agents derives from several facts [2-7] that are briefly described below. The large analogies in ligand-exchange behavior between square-planar complexes of Pt(II) and Au(III), as well as their isoelectronic and isostructural nature represent a main advantage. Worthy to mention also, is the well-known immunomodulatory activity of gold(I) antiarthritic agents, which can be useful, when considering the anticancer activity. Coordination of gold(I) and gold(III) with known antitumour agents is possible and could lead to new compounds with enhanced antitumour activity. In fact, promising antitumour activity for some gold(III) compounds has already been described in literature. Additionally some gold(III) complexes present a good stability in aqueous and physiological environments [8], however, due to the high reduction potential of gold(III), this is not a general rule.

The essential prerequisite for any further pharmaceutical and pharmacological evaluation of gold(III) complexes is to stabilize them. Therefore the right selection of ligands, to achieve such stable complexes, is of great importance.

Arylazopyridine ligands, such as 2-(phenylazo)pyridine (azpy) [9, 10] (Figure 2.1.1), which contain the N=CN=N chromophore, have been studied in the coordination chemistry field for some time. It has been described in the literature that the synthesis of stable chelates is possible with iron(II) [11, 12], rhodium(III) [13, 14], nickel(II) [12], mercury(II) [15], ruthenium(II) [10, 16-25], cobalt(II) and (III) [26, 27], rhenium(V) [28], palladium(II) [29] and platinum(II) [30] salts.

Heteroaromatic compounds comprise an important group of compounds in organic chemistry. By themselves, they are of considerable commercial and practical importance, and are the subject of a voluminous literature [31].

Arylazopyridine ligands are asymmetric heteroaromatic bidentate ligands, which coordinate through the pyridine and aza nitrogen atoms, forming a stable five-membered chelating ring [24]. Arylazopyridine ligands are considered capable of acting both as σ -donor and as π -acceptor. The pyridine ring contributes with its intermediate π -acceptor properties, while its nitrogen is a

Chapter 2

relatively weak σ -donor. The azo group has a low σ -donor ability, but possesses enhanced π -accepting ability through the azo π^* -orbital.

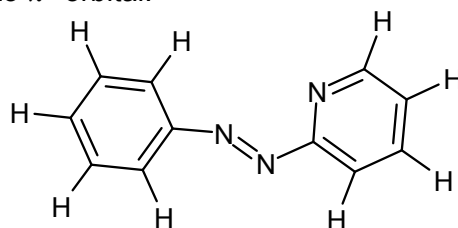


Figure 2.1.1 Schematic representation of 2-(phenylazo)pyridine.

The characteristic red colour of the azo compounds generally arises from an $n\text{-}\pi^*$ -transition located primarily on the azo group. The transition normally centres around 440 nm. There is another transition $\pi\text{-}\pi^*$ in nature, which is due to the aromatic rings involved [19, 32].

The nitrogen forming the pyridine ring, in arylazopyridine ligands, shares the same coordinating properties with the pyridine group in bipyridine (closely related ligand) which means the nitrogen is a weak σ -donor and an intermediate π -acceptor. The azo nitrogen is also a weak σ -donor, but in general, the π -accepting properties of azopyridine ligands are better when compared to bipyridine [25, 33]. Then, the higher π -acidity of azopyridine ligands, in combination with the gold(III) chemical properties, may provide an interesting field to obtain stable coordination compounds with applications in optoelectronic transitions, coordination chemistry and cytotoxic studies.

Developing metal complexes as drugs, however, is not an easy task. Accumulation of metal ions in the body can lead to deleterious effects. Thus, biodistribution and clearance of the metal complex, as well as its pharmacological specificity are to be considered.

Favorable physiological responses of the candidate drugs need to be demonstrated by *in vitro* studies with targeted biomolecules and tissues as well as *in vivo* investigations with xenografts and animal models before they enter clinical trials. A mechanistic understanding of how metal complexes achieve their activities is crucial to their clinical success, as well as to the rational design of new compounds with improved potency. Then, the future development of medicinal inorganic chemistry requires an understanding of the physiological processing of metal complexes, to provide a rational basis for the design of new metal-based drugs.

In this chapter the synthesis and characterization of a series of complexes, with general formula, $[\text{Au}(\text{L})\text{Cl}_2]\text{Cl}$ (where L =2-(phenylazo)pyridine, *o*-tolylazopyridine, 3-methyl-2-phenylazopyridine, 4-methyl-2-phenylazopyridine and 3-methyl-2-tolylazopyridine, Figure 2.1.2) is reported. The ligands selected for this study are derivatized arylazopyridines, containing electron-donating groups, either in the pyridyl moiety, in the phenyl one, or in both, in an attempt to tune the best stability and biological activity.

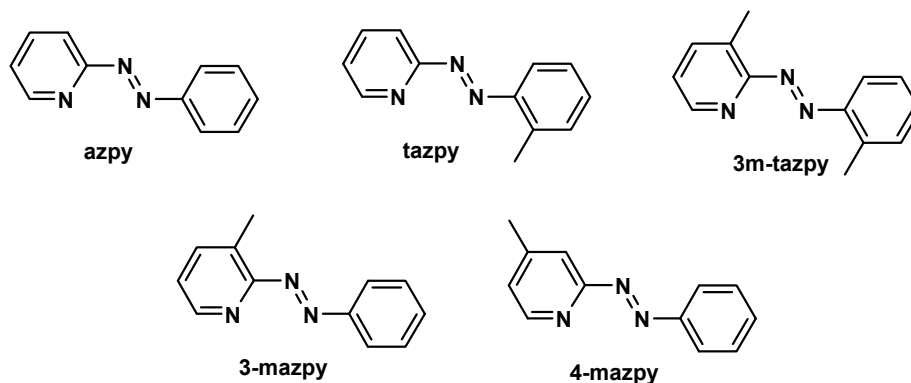


Figure 2.1.2 Schematic representation of the arylazopyridine derivatives used in the synthesis of gold(III) compounds. 2-(phenylazo)pyridine, azpy; *o*-tolylazopyridine, tazpy; 3-methyl-2-tolylazopyridine, 3m-tazpy; 3-methyl-2-phenylazopyridine, 3mazpy; 4-methyl-2-phenylazopyridine and 4mazpy.

The complexes are also designed with two monodentate chloride ligands which could be hydrolyzed and then make 2 sites available for substitution.

In general terms, this research project pursues a better understanding of the chemical, physical and biological behaviour of promising gold complexes and this series of Au(III)-arylazopyridine compounds represent the best current case.

2.2. Experimental description

2.2.1. Methods and instrumental techniques

Chemicals and solvents (analytical reagent grade) were purchased from Acros, Nova-Biochem and Biosolve and used without further purification treatments unless otherwise stated. The 2-aminopyridine, 2-amino-3-picoline and 2-amino-4-picoline were purchased from Fluka while nitrosotoluene and nitrosobenzene were purchased from Sigma-Aldrich. Sodium hydroxide and $\text{HAuCl}_4 \cdot 3\text{H}_2\text{O}$ were purchased from Merck. All other reagents were of high purity and used as purchased without any further purification.

Different techniques were employed in the characterization of the ligands and coordination compounds synthesized. Elemental analyses were performed with a Perkin Elmer series II CHNS/O 2400 Analyzer. Gold concentration was determined with a VISTA-MPX charged-coupled simultaneous ICP-OES spectrometer (inductively coupled plasma optical emission spectrometer), which was measured in mg/L at 242.794 and 267.594 nm. The experiments were carried out in duplicate. Electrospray mass spectra were recorded on a Finnigan TSQ-quantum instrument using an electrospray ionization technique (ESI-MS). The eluent used was the mixture acetonitrile:water 80:20. The UV-visible (UV-Vis) spectra were recorded using a Varian CARY 50 UV/VIS spectrophotometer. NMR experiments were carried out with a Bruker 300 DPX spectrometer. All spectra were recorded at 21 °C, unless otherwise indicated. Temperature was kept constant using a variable temperature unit. The software XWIN-NMR and XWIN-PLOT were used for edition of the NMR spectra. Tetramethylsilane (TMS) or the deuterated solvent residual peaks were used for calibration. In addition 2D ^1H COSY spectra were recorded to confirm the proton assignments. The IR spectra obtained for the products mentioned in this thesis in the 4000-300 cm^{-1} range were recorded as solids with a Perkin Elmer FT-IR Paragon 1000 spectrophotometer using a single-reflection diamond ATR P/N 10500. Conductivity measurements were carried out with a Philips PW9526 digital conductivity meter for freshly prepared 1 mM solutions in nitromethane (AR grade) at 25 °C. The measuring cell consists of two parallel platinum electrodes at a distance of 1 cm.

The absorption spectra in the UV-Vis region were recorded on a Varian CARY 50 UV/VIS spectrophotometer operating at room temperature. The electronic spectra were recorded in freshly prepared acetonitrile solutions due to the poor solubility in water.

2.2.2. Synthetic procedures

2-(phenylazo)pyridine (azpy), 2-(tolylazo)pyridine (tazpy), 2-(phenylazo)-3-methylpyridine (3mazpy), 2-(phenylazo)-4-methylpyridine (4mazpy) and 2-(tolylazo)-3-methylpyridine (3mtazpy): The ligands were prepared as described in the literature [34] with minor modifications in the purification procedure and the characterization results completely agreed with the reported data. Some of the physico-chemical information has not been described in literature before.

In general terms, the ligands were prepared as follows: 5.24g (0.05568 mol) of the corresponding 2-aminopyridine was added to a solution of 26.20g (0.65500 mol) of NaOH in 26.20 mL of water containing 3.41 mL of benzene. Over a 10-min period, 6 g (0.05607) of nitrobenzene (or nitrotoluene) were added with shaking and warmed on a steam bath. After additional 10-min heating, the mixture was extracted with benzene (4x100mL). The benzene fraction was then dried by addition of MgSO_4 , filtrated and finally treated with decolorizing charcoal and then concentrated under reduced pressure to 75 mL. The oily material was passed down a column of alumina and benzene as mobile phase. Complete evaporation of the orange-red fraction produced an oily material which was then added with 100 ml of n-pentane. The mixture was subsequently decanted from a dark brown residue and cooled in dry ice to crystallize. For the synthesis of azpy, nitrosobenzene and 2-aminopyridine were used. The ligand tazpy was synthesised with nitrosotoluene and 2-aminopyridine. For the synthesis of 3mazpy, nitrosobenzene and 2-amino-3-picoline were used. 4mazpy was synthesised with nitrosobenzene and 2-amino-4-picoline and finally for the synthesis of 3mtazpy, nitrosotoluene and 2-amino-3-picoline were used.

2-(phenylazo)pyridine (azpy): Elemental analysis for $C_{11}H_9N_3$: Calculated (%): C, 72.11; N, 22.94 and H, 4.95. Found (%): C, 71.92; N, 23.12 and H, 5.01. mp: 32-34 °C. ESI-MS: $m/z=183.48$, $C_{11}H_9N_3$, where calculated $m/z=183.21$. IR: 3056, 1580-1570, 1490-1432, 1420, 788-736 and 684 cm^{-1} . UV-Vis in acetonitrile ($\lambda_{max}(\log\epsilon_M)$): 220(4.19), 315(4.34) and 450(2.60). 1H NMR (300 MHz, acetone, 294 K, s=singlet, d=doublet, t=triplet, dd=double doublet and m=multiplet): $\delta=8.720$ (d, 1H, H_6), 7.996(m, 3H, H_4 and $2H_o$), 7.765 (d, 1H, H_3), 7.619 (m, 3H, $2H_m$ and H_p) and 7.531 ppm (dd, 1H, H_5).

2-(tolylazo)pyridine (tazpy): Elemental analysis for $C_{12}H_{11}N_3$: Calculated (%): C, 73.07; N, 21.30 and H, 5.62. Found (%): C, 72.99; N, 20.90 and H, 5.85. mp: 39-41 °C. ESI-MS: $m/z=197.95$, $C_{12}H_{11}N_3$, where calculated $m/z=197.24$. IR: 3080-2960, 1596-1572, 1476-1455, 1414, 1304-1148, 1046-960, 788-716 and 620-407 cm^{-1} . UV-Vis in acetonitrile ($\lambda_{max}(\log\epsilon_M)$): 320(4.20) and 454(2.33). 1H NMR (300 MHz, acetonitrile, 294 K, s=singlet, d=doublet, t=triplet and m=multiplet): $\delta=8.692$ (d, 1H, H_6), 7.951 (t, 1H, H_4), 7.685 (m, 2H, H_3 and H_o), 7.444 (m, 3H, H_5 , H_{m1} and H_p), 7.316 ppm (t, 1H, H_{m2}) and 2.716 (s, 3H, CH_3o).

2-(phenylazo)-3-methylpyridine (3mazpy): Elemental analysis for $C_{12}H_{11}N_3$: Calculated (%): C, 73.07; N, 21.30 and H, 5.62. Found (%): C, 73.02; N, 20.87 and H, 5.97. mp: 30-34 °C. ESI-MS: $m/z=197.95$, $C_{12}H_{11}N_3$, where calculated $m/z=197.24$. IR: 3055-2980, 1573, 1478-1406, 1112, 792-755, 686 and 576-531 cm^{-1} . UV-Vis in acetonitrile ($\lambda_{max}(\log\epsilon_M)$): 224(3.86), 319(3.93) and 453(2.66). 1H NMR (300 MHz, acetonitrile, 294 K, s=singlet, d=doublet, t=triplet, dd=double doublet and m=multiplet): $\delta=8.414$ (d, 1H, H_6), 7.955(m, 2H, H_o), 7.794 (d, 1H, H_4), 7.576 (m, 3H, $2H_m$ and H_p), 7.359 ppm (dd, 1H, H_5) and 2.586 (s, 3H, CH_{3py}).

2-(phenylazo)-4-methylpyridine (4mazpy): Elemental analysis for $C_{12}H_{11}N_3$: Calculated (%): C, 73.07; N, 21.30 and H, 5.62. Found (%): C, 72.91; N, 21.49 and H, 5.89. mp: 46-48 °C. ESI-MS: $m/z=197.97$, $C_{12}H_{11}N_3$, where calculated $m/z=197.24$. IR: 3054-2900, 1598-1564, 1490-1445, 1383, 1309-1070, 992, 834-684, 501 and 448 cm^{-1} . UV-Vis in acetonitrile ($\lambda_{max}(\log\epsilon_M)$): 225(3.24), 316(3.37) and 450(2.58). 1H NMR (300 MHz, acetonitrile, 294 K, s=singlet, d=doublet, t=triplet and m=multiplet): $\delta=8.535$ (d, 1H, H_6), 7.953 (m, 2H, $2H_o$), 7.582 (m, 4H, H_3 , $2H_m$ and H_p), 7.532 ppm (d, 1H, H_5) and 2.444 (s, 3H, CH_{3py}).

2-(tolylazo)-3-methylpyridine (3mtazpy): Elemental analysis for $C_{13}H_{13}N_3$: Calculated (%): C, 73.91; N, 19.89 and H, 6.20. Found (%): C, 73.91; N, 20.00 and H, 6.46. mp: 49-52 °C. ESI-MS: $m/z=315.90$, $2C_{13}H_{13}N_3 \cdot 5CH_3CN$ (base peak); 211.93, $C_{13}H_{13}N_3$, where calculated $m/z=211.27$. IR: 3050-2927, 1610-1560, 1480-1377, 1278-1156, 1116, 801-712 585-561 and 489-420 cm^{-1} . UV-Vis in acetonitrile ($\lambda_{max}(\log\epsilon_M)$): 230(3.88), 325(4.10) and 465(2.75). 1H NMR (300 MHz, acetonitrile, 294 K, s=singlet, d=doublet, t=triplet and m=multiplet): $\delta=8.412$ (d, 1H, H_6), 7.794(d, 1H, H_4), 7.597 (d, 1H, H_o), 7.434 (m, 2H, H_{m1} and H_p), 7.333 ppm (m, 2H, H_{m2} and H_5), 2.688(s, 3H, CH_3o) and 2.564 (s, 3H, CH_{3py}).

Dichlorido{2-(phenylazo)pyridine}gold(III) chloride dihydrate, $[Au(azpy)Cl_2]Cl \cdot 2H_2O$

(abbreviated: Au-azpy): The compound was synthesized according to the following procedure. 0.05g (0.127 mmol) of $HAuCl_4 \cdot 3H_2O$ was added to a solution of 0.00070g (0.0165 mmol) of LiCl in 2.5 mL of dichloromethane and one drop of methanol. A solution of the corresponding ligand, 2-(phenylazo)pyridine (0.025g, 0.136 mmol), in 2.5 mL of dichloromethane was added to the gold solution. The system was kept under reflux for 1 h. The solid formed after this time was collected by filtration, washed plenty with dichloromethane and cold water and dried with hexane and dry diethyl ether. Yield: 58.78 % (0.07465 mmol, 0.03901 g). Elemental analysis for $AuC_{11}H_9N_3Cl_3O_2$: Calculated (%): C, 25.28; N, 8.04; H, 2.51 and Au, 37.69. Found (%): C, 25.23; N, 8.15; H, 2.09 and Au, 36.7. ESI-MS: $m/z=472.30$, $\{2[Au(azpy)Cl_2] \cdot (CH_3CN)\}^{2+}$, where calculated $m/z=471.6$. IR: 3350-2900, 1616-1592, 1526-1460, 1432, 781, 678, 537-522 and 352 cm^{-1} . UV-Vis in acetonitrile ($\lambda_{max}(\log\epsilon_M)$): 225(4.782), 335(4.386) and 440(2.87). 1H NMR (300 MHz, acetone, 294 K, s=singlet, d=doublet, t=triplet and m=multiplet): $\delta=9.24620$ (d, 1H, H_6), 9.02453(t, 1H, H_4), 8.66925

(d, 1H, H₃), 8.38438 (t, 1H, H₅), 8.14607(m, 2H, H_o) and 7.77802 ppm (m, 3H, 2H_m and H_p). $\Lambda_M(\text{CH}_3\text{NO}_2)=86 \Omega^{-1}\text{cm}^2\text{mol}^{-1}$.

Dichlorido{2-(tolylazo)pyridine}gold(III) chloride dihydrate, [Au(tazpy)Cl₂]Cl•2H₂O

abbreviated: Au-tazpy): The compound was synthesized following a similar procedure as the one used in the synthesis of *Au-azpy*. 0.05g (0.127 mmol) of H₂AuCl₄•3H₂O was added to a solution of 0.00070g (0.0165 mmol) of LiCl in 2.5 mL of dichloromethane and one drop of methanol. A solution of the corresponding ligand, 2-(tolylazo)pyridine (0.0263 g, 0.133 mmol), in 2.5 mL of dichloromethane was added to the gold solution. The system was kept under reflux for 1 h. The solid formed after this time was collected by filtration, washed plenty with dichloromethane and cold water and dried with hexane and dry diethyl ether. Yield: 72.37 % (0.09191 mmol, 0.04932 g). Elemental analysis for AuC₁₂H₁₅N₃Cl₃O₂: Calculated (%): C, 26.86; N, 7.83; H, 2.82 and Au, 36.71. Found (%): C, 26.85; N, 7.80; H, 2.92 and Au, 36.9. ESI-MS: m/z=465.95, [Au(tazpy)Cl₂]¹⁺, where calculated m/z=465.11. IR: 3250, 3100-2900, 1623-1575, 1520-1475, 1414, 1339-1194, 1154, 899, 780-719, 544, 491, and 352 cm⁻¹. UV-Vis in acetonitrile ($\lambda_{\text{max}}(\log \epsilon_M)$): 227(4.69), 332(4.24) and 462(2.95). ¹H NMR (300 MHz, acetonitrile, 294 K, s=singlet, d=doublet, t=triplet and m=multiplet): δ =8.783 (m, 2H, H₆ and H₄), 8.507(d, 1H, H₃), 8.122 (t, 1H, H₅), 7.844 (d, 1H, H_o), 7.670 (t, 1H, H_p), 7.552 ppm (d, 1H, H_{m1}), 7.417 ppm (d, 1H, H_{m2}) and 2.839 ppm (s, 3H, CH_{3o}).

Dichlorido{2-(phenylazo)-3-methylpyridine}gold(III) chloride trihydrate, [Au(3mazpy)Cl₂]Cl•3H₂O (abbreviated: Au-3mazpy)

The title compound was synthesized following a similar procedure as the one used in the synthesis of *Au-azpy* and *Au-tazpy*, the only difference is the reaction solvent used: 0.05g (0.127 mmol) of H₂AuCl₄•3H₂O was added to a solution of 0.0044g (0.104 mmol) of LiCl in 2.5 mL of water. A suspension of the corresponding ligand, 2-(phenylazo)-3-methylpyridine (0.0263 g, 0.133 mmol), in 2.5 mL of water and a few drops of acetone were added to the gold solution. After interaction of the ligand suspension and the gold solution a homogeneous orange solution was obtained. After 5 minutes under reflux a yellow solid appeared, but spontaneously redissolved after some more minutes. The system was kept under reflux for another 45 min when a dark orange solid suspended was evident. The solid formed after this time was collected by filtration, washed extensively with dichloromethane and cold water and dried with hexane and dry diethyl ether. Yield: 56.52 % (0.07178 mmol, 0.03981 g). Elemental analysis for AuC₁₂H₁₇N₃Cl₃O₃: Calculated (%): C, 25.99; N, 7.58; H, 3.09 and Au, 35.51. Found (%): C, 25.99; N, 7.56; H, 2.85 and Au, 35.93. ESI-MS: m/z=465.66, [Au(3mazpy)Cl₂]¹⁺; 485.81, {2[Au(3mazpy)Cl₂](CH₃CN)}²⁺; 501.14, {[Au(3mazpy)Cl₂]¹⁺•2H₂O}, where calculated m/z values are 465.11, 485.61, and 501.11 respectively. IR: 3250, 3104-2900, 1600-1582, 1490-1404, 1306-1270, 1223 1158-1134, 1071, 790-743, 684, 552, 500 and 356 cm⁻¹. UV-Vis in acetonitrile ($\lambda_{\text{max}}(\log \epsilon_M)$): 225(4.35), 343(4.33) and 472(2.70). ¹H NMR (300 MHz, acetonitrile, 294 K, s=singlet, d=doublet, t=triplet and m=multiplet): δ =8.949 (d, 1H, H₆), 8.266(m, 3H, 2H_o and H₄), 7.748 ppm (m, 4H, H₅, 2H_m and H_p) and 2.794 ppm (s, 3H, CH_{3py}).

Dichlorido{2-(phenylazo)-4-methylpyridine}gold(III) chloride, [Au(4mazpy)Cl₂]Cl

(abbreviated: Au-4mazpy): The title compound was synthesized following the same procedure used in the synthesis of *Au-3mazpy*: 0.05g (0.127 mmol) of H₂AuCl₄•3H₂O was added to a solution of 0.0044g (0.104 mmol) of LiCl in 2.5 mL of water. A suspension of the corresponding ligand, 2-(phenylazo)-4-methylpyridine (0.0263 g, 0.133 mmol), in 2.5 mL of water and a few drops of acetone was added to the gold solution. After interaction of the ligand suspension and the gold solution a homogeneous orange solution was obtained. After 1 minute under reflux a yellow solid appeared, which redissolved after some more minutes. The system was kept under reflux for another 15 min when a dark orange solid suspended was evident. The solid formed after this time was collected by filtration, washed extensively with dichloromethane and cold water and dried with hexane and dry diethyl ether. Yield: 63.34 % (0.08045 mmol, 0.04027 g). Elemental analysis for AuC₁₂H₁₁N₃Cl₃: Calculated (%): C, 28.79; N, 8.39; H, 2.21 and Au, 39.35. Found (%): C, 28.77; N, 8.39; H, 1.97 and Au, 39.98. ESI-MS: m/z=500.72, [Au(4mazpy)Cl₂]Cl; 483.80, [Au(4mazpy)Cl₂]¹⁺•H₂O; 465.62, [Au(4mazpy)Cl₂]¹⁺, where calculated m/z values are 500.57, 483.13 and 465.11 respectively. IR: 3042, 1616-1558, 1486, 1399, 1314-1255, 1200-1116, 1046, 902, 827-683, 584, 527-460, and 358 cm⁻¹. UV-Vis in acetonitrile ($\lambda_{\text{max}}(\log \epsilon_M)$): 225(4.54),

334(4.29) and 441(2.70). ^1H NMR (300 MHz, acetonitrile, 294 K, s=singlet, d=doublet, t=triplet and m=multiplet): δ =8.859 (s, 1H, H₆), 8.155(d, 2H, H_o), 7.998 (d, 1H, H₃), 7.72 (m, 4H, H₅, 2H_m and H_p) and 2.632 ppm (s, 3H, CH_{3py}).

Dichlorido{2-(tolylazo)-3-methylpyridine}gold(III) chloride trihydrate, [Au(3mtazpy)Cl₂]Cl

•3H₂O (abbreviated: **Au-3mtazpy**): The compound was synthesized following a similar procedure as the one used in the synthesis of *Au-3mazpy* and *Au-4mazpy*. 0.05g (0.127 mmol) of H₂AuCl₄·3H₂O was added to a solution of 0.0044g (0.104 mmol) of LiCl in 2.5 mL of water. A suspension of the corresponding ligand, 2-(tolylazo)-3-methylpyridine (0.02814 g, 0.133 mmol), in 2.5 mL of water and a few drops of acetone was added to the gold solution. After interaction of the ligand suspension and the gold solution a homogeneous orange solution was obtained. After 5 minute under reflux a yellow solid appeared which redissolved after some more minutes. The system was kept under reflux for another 25 min when a dark orange solid suspended was evident. The solid formed after this time was collected by filtration, washed extensively with dichloromethane and cold water and dried with hexane and dry diethyl ether. Yield: 79.12 % (0.10049 mmol, 0.05895 g). Elemental analysis for AuC₁₃H₂₁N₃Cl₃O₄: Calculated (%): C, 26.62; N, 7.16; H, 3.61 and Au, 33.57. Found (%): C, 26.61; N, 7.13; H, 3.95 and Au, 34.08. ESI-MS: m/z=532.86, [Au(4mazpy)Cl₂]Cl·H₂O; 514.72, [Au(4mazpy)Cl₂]Cl; 479.65, [Au(4mazpy)Cl₂]¹⁺, where calculated m/z values are 532.59, 514.59 and 479.14 respectively. IR: 3200, 3102, 1594-1558, 1478-1436, 1403, 1280-1107, 1036, 926, 771, 707, 594 and 357 cm⁻¹. UV-Vis in acetonitrile ($\lambda_{\text{max}}(\log \epsilon_{\text{M}})$): 225(4.46), 347(4.16) and 484(2.94). ^1H NMR (300 MHz, acetonitrile, 294 K, s=singlet, d=doublet, t=triplet and m=multiplet): δ =8.924 (d, 1H, H₆), 8.278 (d, 1H, H₄), 7.843 (d, 1H, H_o), 7.771 (m, 1H, H₅), 7.629 (t, 1H, H_{m2}), 7.537 (d, 1H, H_{m1}), 7.414 (t, 1H, H_p), 2.862(s, 3H, CH_{3o}) and 2.707 ppm (s, 3H, CH_{3py}).

2.3. Results and discussion

2.3.1 Synthesis and characterization

2.3.1.1. Synthesis and characterization of the 2-(arylazo)pyridine ligands

The preparation of the 2-(arylazo)pyridine ligands, azpy, tazpy, 3mazpy, 4mazpy and 3mtazpy, was achieved applying reported procedures [9, 10, 24, 34]. The azo group joins together aromatic rings, resulting in an extended system of conjugated multiple bonds. In general, azo compounds are synthesized by first reacting a primary aromatic amine with nitrous acid, HNO₂, to produce an aryldiazonium ion, Ar-N⁺≡N. This ion can subsequently couple with a nucleophilic aromatic compound, such as an aryl amine or a phenol, to produce the azo compound.

In the particular case of the ligands presented in this thesis, they were prepared by condensation of the corresponding nitrosobenzene or nitrosotoluene, in alkaline solution, with 2-amino-3-picoline, 2-amino-4-picoline or 2-aminopyridine, respectively (Figure 2.1.3). Specific details in the synthesis and isolation are described in the experimental section.

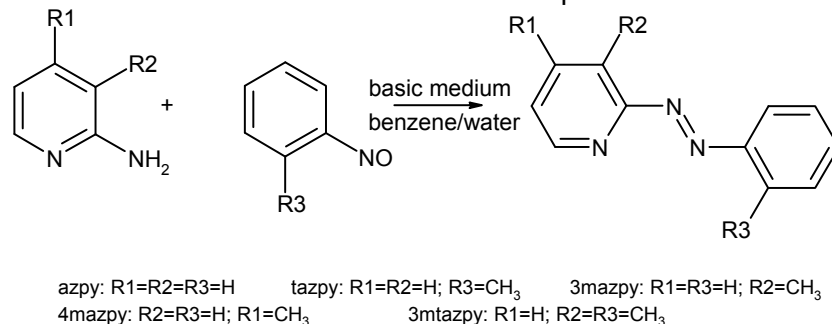


Figure 2.3.1 Schematic representation of the synthetic procedure for 2-(arylazo)pyridine ligands.

Workup by column chromatography on alumina was necessary to isolate these ligands in high purity and they were obtained as red or deep orange solids in yields from 51-78%. All five 2-(arylazo)pyridine derivatives synthesised were found to be air-stable and soluble in common organic solvents. The molecular formulae of the ligands synthesised were established with the help of IR, MS, UV-Vis and NMR spectroscopies, microanalytical data and melting points. Most of

Chapter 2

the information presented here was not available in literature, and just for the case of azpy, comparison with reported data was possible [10, 20, 22, 24, 35]. For all cases, the spectroscopic properties are in accordance with their formulation and the relevant data is summarized in table 2.3.1 and figure 2.3.2.

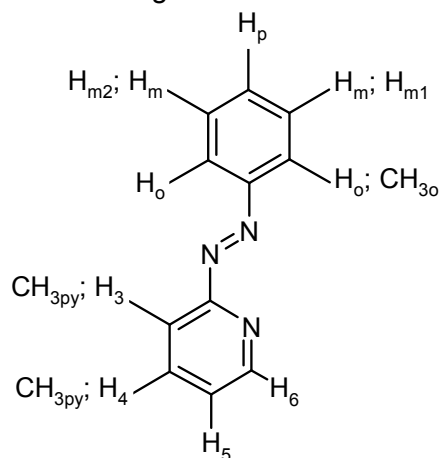


Figure 2.3.2 Schematic representation of 2-(arylo)pyridine ligands with the numbering used in the assignment of the resonance peaks.

Table 2.3.1 Spectroscopic data for the ligands.

Ligand	IR (ν N=N, cm^{-1}) ^a	¹ H NMR ^b	ESI-MS (m/z) ^c
azpy	1420	8.720 (d, 1H, H ₆), 7.996(m, 3H, H ₄ and 2H _o), 7.765 (d, 1H, H ₃), 7.619 (m, 3H, 2H _m and H _p) and 7.531 ppm (dd, 1H, H ₅)	183.48(183.21)
tazpy	1414	8.692 (d, 1H, H ₆), 7.951 (t, 1H, H ₄), 7.685 (m, 2H, H ₃ and H _o), 7.444 (m, 3H, H ₅ , H _{m1} and H _p), 7.316 ppm (t, 1H, H _{m2}) and 2.716 (s, 3H, CH ₃ O)	197.95(197.24)
3mazpy	1438	8.414 (d, 1H, H ₆), 7.955(m, 2H, H _o), 7.794 (d, 1H, H ₄), 7.576 (m, 3H, 2H _m and H _p), 7.359 ppm (dd, 1H, H ₅) and 2.586 (s, 3H, CH ₃ py)	197.95(197.24)
4mazpy	1446	8.535 (d, 1H, H ₆), 7.953 (m, 2H, 2H _o), 7.582 (m, 4H, H ₃ , 2H _m and H _p), 7.532 ppm (d, 1H, H ₅) and 2.444 (s, 3H, CH ₃ py)	197.97(197.24)
3mtazpy	1453	8.412 (d, 1H, H ₆), 7.794(d, 1H, H ₄), 7.597 (d, 1H, H _o), 7.434 (m, 2H, H _{m1} and H _p), 7.333 ppm (m, 2H, H _{m2} and H ₅), 2.688(s, 3H, CH ₃ O) and 2.564 (s, 3H, CH ₃ py)	211.93(211.27)

^a Solid, ^b In CH₃CN deuterated, 294 K, s=singlet, d=doublet, t=triplet, dd=double doublet and m=multiplet, ^c Simulated masses are presented in parenthesis

Data as the melting point, that it is normally used as a criterion of purity, in case of azpy was 32-34 °C in agreement with published values. Higher melting points values were observed for the other ligands described here within small ranges (see experimental section).

All the compounds display molecular ion envelopes of high to medium intensity in their positive ESI mass spectra, confirming the nature of all ligands. Fragmentation ions were observed, where interaction with solvent could be proposed, as well as the presence of starting materials. All the peaks exhibited the correct isotopomer distribution (spectrum of azpy is shown in figure 2.3.3).

IR spectra of azpy, tazpy, 3mazpy, 4mazpy and 3mtazpy displayed characteristic frequencies in the range 4000-400 cm^{-1} . A complete assignment of all the peaks is not achieved due to the complexity of the spectra but some vibrations could be associated with some functional groups present in the ligands. The important functional groups C=N, C=C and N=N stretching modes were observed in this range. From IR data, azpy showed the N=N stretching vibration at 1420 cm^{-1} (in agreement with reported values by Krause [10], Hotze [24] and Sahavisit [36]), whereas the N=N stretching mode of tazpy appeared at 1414 cm^{-1} . This indicates that the electron density delocalized into the π^* -orbital of the azo function in tazpy was found to be slightly larger than the one observed in azpy, due to the presence of the substituent methyl group at the *ortho* position on the tolyl ring. The opposite effect is observed when electron-donating methyl groups are placed in the pyridyl moiety of the 2-(arylo)pyridine, as could be confirmed by the frequency values observed for the N=N stretching mode in the IR spectra of 3mazpy and 4mazpy.

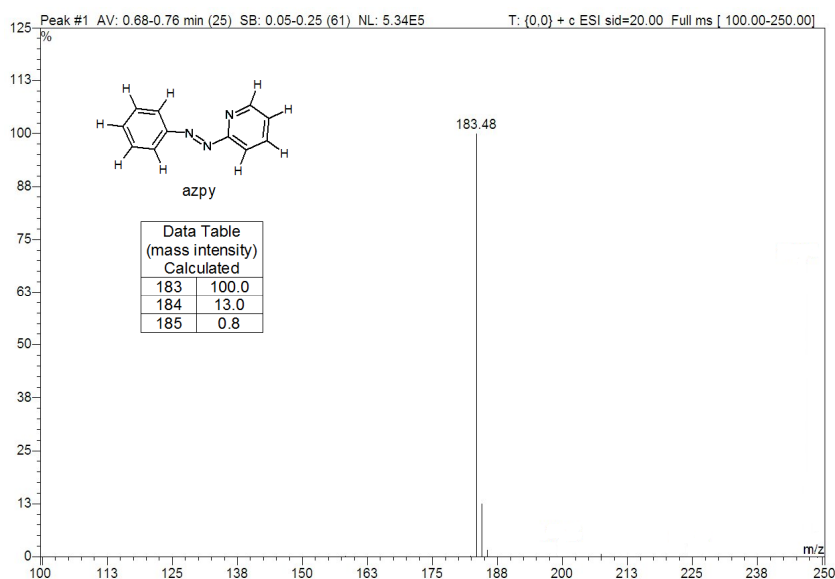


Figure 2.3.3 ESI-MS positive ion spectrum from azpy (m/z in Da). The calculated data is concentrated in the table.

In general terms, the intensity of the peaks has been related to lack of symmetry as a result of the different nature of the two aromatic rings conjugated in 2-(aryloxy)pyridine structure. Other important peaks related to the aromatic nature of these ligands are localized in the frequency range of $790\text{--}650\text{ cm}^{-1}$. The pattern of substitution (mono- and *ortho*-) in the aromatic rings could be described by the peaks located in this range. Intense bands around 684 cm^{-1} are considered as a result of the vibration modes in the mono substituted ring. The intense peak at 736 cm^{-1} in azpy is generated by the vibration modes in the *ortho*-substituted pyridine. The $\nu(\text{C-H})$ vibration of the methyl groups in tazpy, 3mazpy, 4mazpy and 3mtazpy are detected around $3080\text{--}2900\text{ cm}^{-1}$ (data reported in the experimental section). The assignments of selected bands and frequencies are summarized on table 2.3.2.

Table 2.3.2 Selected IR assignment of 2-(aryloxy)pyridine ligands.

Peaks	Frequencies (cm^{-1})				
	azpy	tazpy	3mazpy	4mazpy	3mtazpy
$\nu\text{ C=N}$	1580-1570s	1596-1572s	1573-1560m	1598-1564s	1610-1560m
$\nu\text{ C=N, } \nu\text{ C=C}$	1490-1430s	1476-1455s	1478-1406s	1490-1445m	1480-1377s
$\nu\text{ N=N}$	1420 vs	1414 s	1438 s	1446m	1453vs
ring breathing mode	1331-1297 m	1304-1279m	1331-1305m	1383-1298s	1304-1278m
ring mono substitution	991 m	989m	931w	992m	1041m
$\delta\text{ =N-C=}$	788-736 vs	788-716 vs	792-755 vs	834-738vs	801-712 vs
	684 vs	not present	686 vs	684vs	not present

^1H NMR spectroscopy represents a valuable tool for the characterization of these organic compounds. From the ^1H NMR spectra of the ligands discussed here, several patterns are observed. In all cases, the clean spectrum indicates a high purity of the samples. The assignment of each peak was obtained through the integration values, multiplicity of signals, deshielding effect in the hydrogen atoms close to the nitrogen in the pyridine ring and 2D ^1H COSY experiments.

The ^1H NMR spectra of all the ligands show the pyridine-ring protons at *ortho* position (H_6) experiencing a downfield shift in the chemical shift values. The integral ratio between the peaks also correlates with the chemical structure proposed in all cases.

For instance, the H_6 doublet of azpy has been assigned on account of the ^3J coupling (typical values of around 5Hz for the H_6 versus around 9 Hz for the H_3 doublet, as concluded from selective substitution of the pyridine-ring protons) and the further assignments of the H_4 and H_5 were made on the basis of 2D ^1H COSY experiments as the three pyridine protons, H_6 , H_5 and H_4 are mutually coupled with each other. It was also considered that the broadness in the H_6 peak is attributed to the nitrogen magnetic environment. The appearance of H_6 at relatively low field could be explained by the deshielding effect of the pyridine nitrogen next to this proton. The ^1H NMR spectrum from azpy and the corresponding assignment of peaks is condensed in figure 2.3.4. Worthy mentioning is the deshielding effect observed in H_6 , which is generated by the vicinal

nitrogen atom in the azo moiety which maintains a partial positive charge. The absence of a single peak for the protons H_o , H_m and H_p in the spectrum indicates a reduced symmetry for the phenyl moiety, which could be generated by the azo moiety or some intermolecular interactions [35].

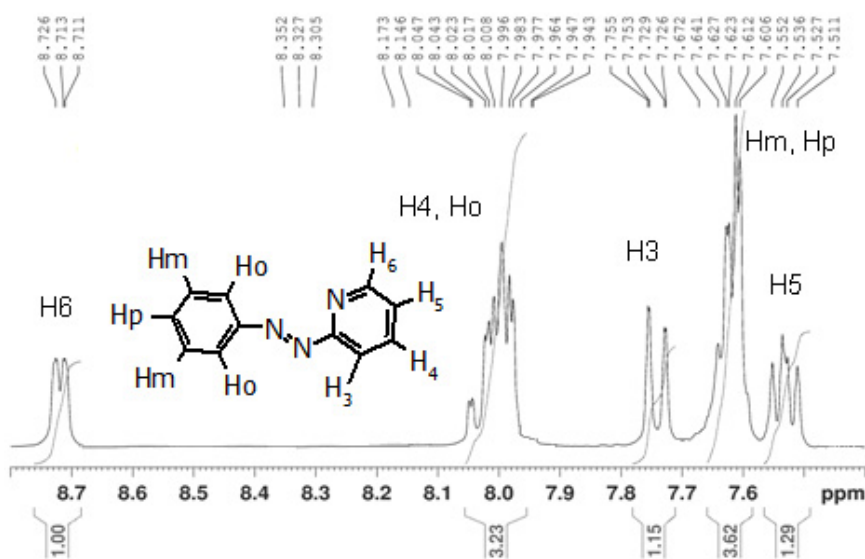


Figure 2.3.4 ^1H NMR spectrum in the aromatic region for azpy in deuterated acetone.

The spectra and the corresponding assignment of resonance peaks for the ligands tazpy, 3mazpy, 4mazpy and 3mtazpy are described in detail in figure 2.3.5.

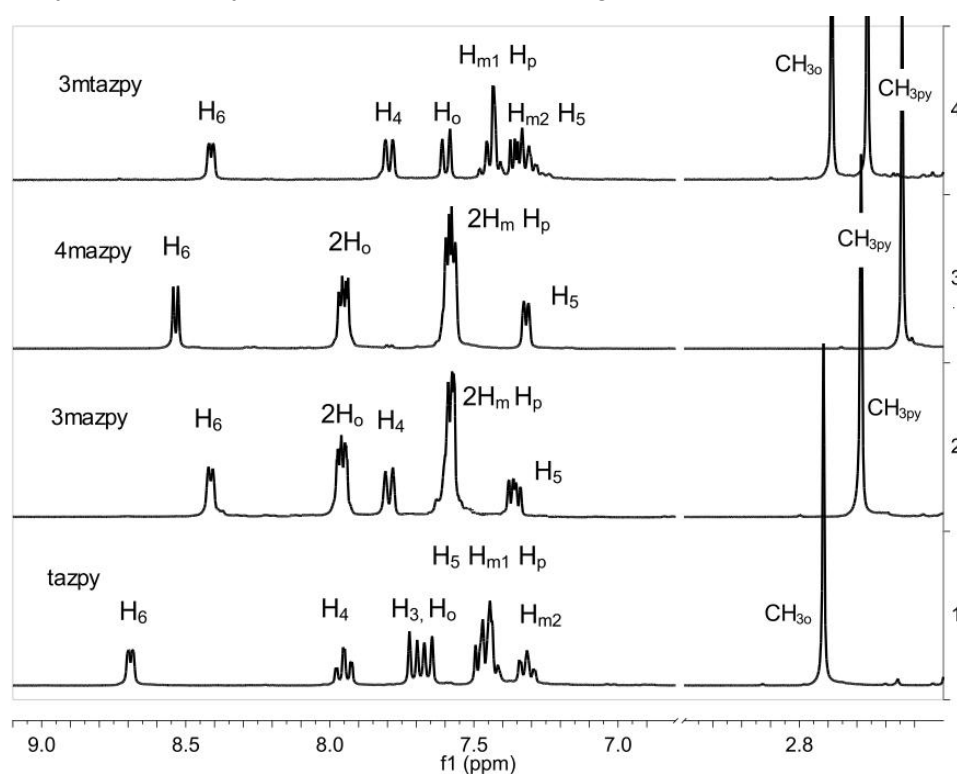


Figure 2.3.5 ^1H NMR spectra of 2-(arylo)pyridine ligands in deuterated acetonitrile at 294 K. For the assignment and numbering the reader is referred to figure 2.3.2.

The introduction of a methyl group has a considerable effect on the π -electron density in the heterocyclic rings and thus in the chemical shifts. For instance, the protons in 3mazpy and 4mazpy are slightly shifted upfield with respect to the parent compound, azpy, especially the protons at *para* position with respect to the methyl group. Such effect has been observed in pyridine, furan and pyrrole families [37, 38]. This is clearly the result of the increased π -electron density in the heterocyclic ring due to the presence of the methyl groups. The effect is slightly higher when the methyl group is located in the phenyl moiety instead of the pyridyl moiety, as

Chapter 2

observed in case of tazpy and 3mtazpy. Finally the upfield shift effect in 3mtazpy is intermediate between the higher shift in 3mazpy and the lower effect in tazpy, a behaviour that could be predicted.

The absorption spectra of all the 2-(arylzo)pyridine ligands in the UV-Vis region were recorded using a Varian CARY 50 UV/VIS spectrophotometer operating at room temperature. The electronic spectra had to be recorded in freshly prepared acetonitrile solutions, due to the poor solubility in water. The characteristic spectrum of 2-(arylo)pyridine ligands presents intense peaks in the region that comprises 200-550 nm [35]. The UV-Vis spectra of all compounds is essentially consisting of $\pi \rightarrow \pi^*$ -transitions in the range 220-326 nm with high molar absorption coefficients and $n \rightarrow \pi^*$ -bands around 455 nm with smaller molar absorption coefficients. The detailed information is fully described in the experimental section and the UV-Vis spectra of the ligands are depicted in figures 2.3.6 and 2.3.7.

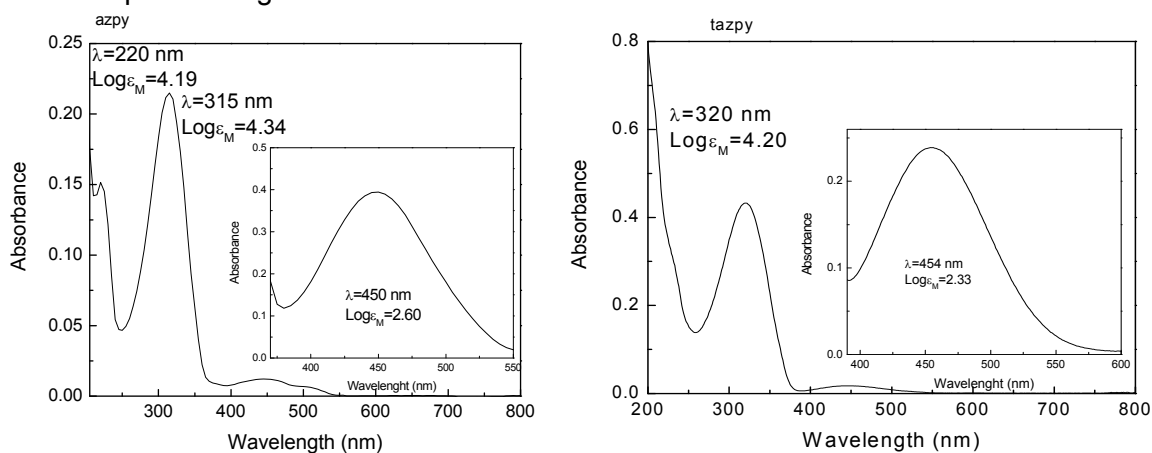


Figure 2.3.6 UV-Vis spectra of azpy and tazpy in acetonitrile at 294 K; the inset shows a vertically expanded view of the spectra (higher concentration) in the visible region.

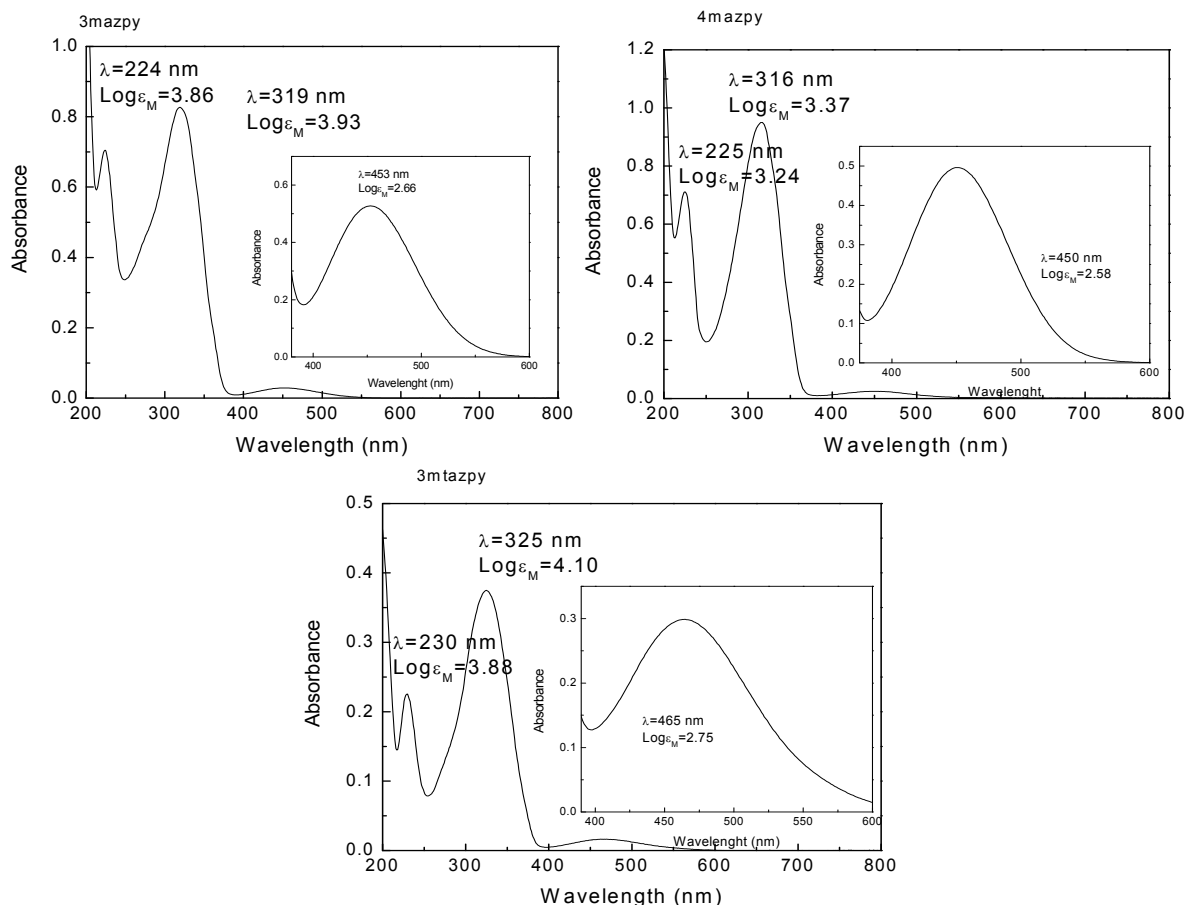
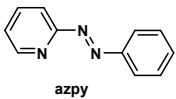
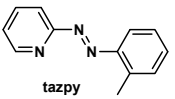
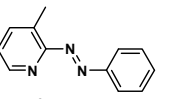
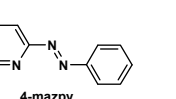
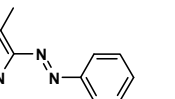


Figure 2.3.7 UV-Vis spectra of 3mazpy, 4mazpy and 3mtazpy in acetonitrile at 294 K; the inset shows a vertically expanded view of the spectra (higher concentration) in the visible region.

Chapter 2

Important to notice again is the influence of the methyl moiety in the electronic spectra. When the methyl group is attached to the phenyl moiety, at the *ortho* position, a significant bathochromic shift is observed in the intraligand charge-transfer transitions as clearly visible in the case of tazpy and 3mtazpy. This effect could be explained as a result of the increased π -electron density, although interactions with the solvent could not be discharged. The influence of an increased electron density due to substitution of a methyl moiety is less pronounced in the pyridine ring, as has been observed in 3mazpy and 4mazpy. The increased electron density in tazpy, 3mazpy, 4mazpy and 3mtazpy produce little effect in the molar absorption coefficients (table 2.3.3).

Table 2.3.3 Electronic spectral data for the 2-(arylo)pyridine ligands.

Transitions nature	Wavelength [$\log \epsilon_M$] (nm)				
					
$\pi \rightarrow \pi^*$	220[4.19]	-	224[3.86]	225[3.24]	230[3.88]
$\pi \rightarrow \pi^*$	315[4.34]	320[4.20]	319[3.93]	316[3.37]	325[4.10]
$n \rightarrow \pi^*$	450[2.60]	454[2.33]	453[2.66]	450[2.58]	465[2.75]

2.3.1.2. Synthesis and characterization of 2-(arylo)pyridine gold(III) complexes

The complexes were prepared according to the procedures detailed in the experimental section. The establishment of the best experimental conditions was achieved through several experiments and analysis of the products. In general terms, the complexes were synthesised using two different experimental conditions. In case of Au-azpy and Au-tazpy, the synthesis were achieved when stoichiometric amounts of starting materials were dissolved and reacted in dichloromethane, as schematically described in figure 2.3.8.

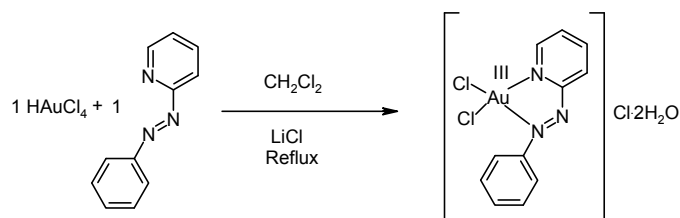


Figure 2.3.8 Synthetic scheme of Au-azpy compound (experimental section contains a detail description of the synthetic procedure).

For the synthesis of Au-3mazpy, Au-4mazpy and Au-3mtazpy, closely related experimental conditions were applied, as in these cases, instead of dichloromethane, a water-acetone medium offered better results. When the synthesis of these complexes was achieved in dichloromethane, the formation of metallic gold and several byproducts was found to be a problem, and purification processes were not successful.

Even though all the complexes are quite stable in the solid state and could be stored for months without appreciable change, protection for light and humidity is strongly recommended. All compounds are orange or yellow in colour and generally soluble in common polar organic solvents, such as methanol, acetone, acetonitrile, dimethylformamide (dmf) or dimethylsulfoxide (dmsO) and just slightly soluble in water.

The elemental analyses were found in agreement with the proposed structures and stressed the purity of the samples. The yields afforded were in the range of 50-79%. The conductance measurements, recorded in nitromethane at 25 °C, indicate that the complexes dissociate in the solvent and behave as 1:1 electrolytes [39].

ESI mass spectroscopy probes to be a useful technique for characterization of the complexes. The ESI-mass spectrum of Au-azpy exhibits the major positive peaks at $m/z = 472.30$,

Chapter 2

and 474.30, which corresponds to the cationic structure, $\{2[\text{Au}(\text{azpy})\text{Cl}_2](\text{CH}_3\text{CN})\}^{2+}$. The ratio of the peaks, which is a distinct pattern for the presence of 2 chlorine atoms (natural isotopes ^{35}Cl and ^{37}Cl , with an abundance 75.77/24.23%) confirms the presence of 2 chlorine atoms in the molecular fragment (see Figure 2.3.9). In figure 2.3.10, an expansion of the complex peak is presented. A mixture of $\text{CH}_3\text{CN}/\text{H}_2\text{O}$, 80:20 was used as eluent. A fragmentation ion was observed at $m/z = 183.52$, which corresponds to the free azpy ligand. All the peaks exhibited the correct isotopomer distribution mainly derived from the number of chlorine atoms.

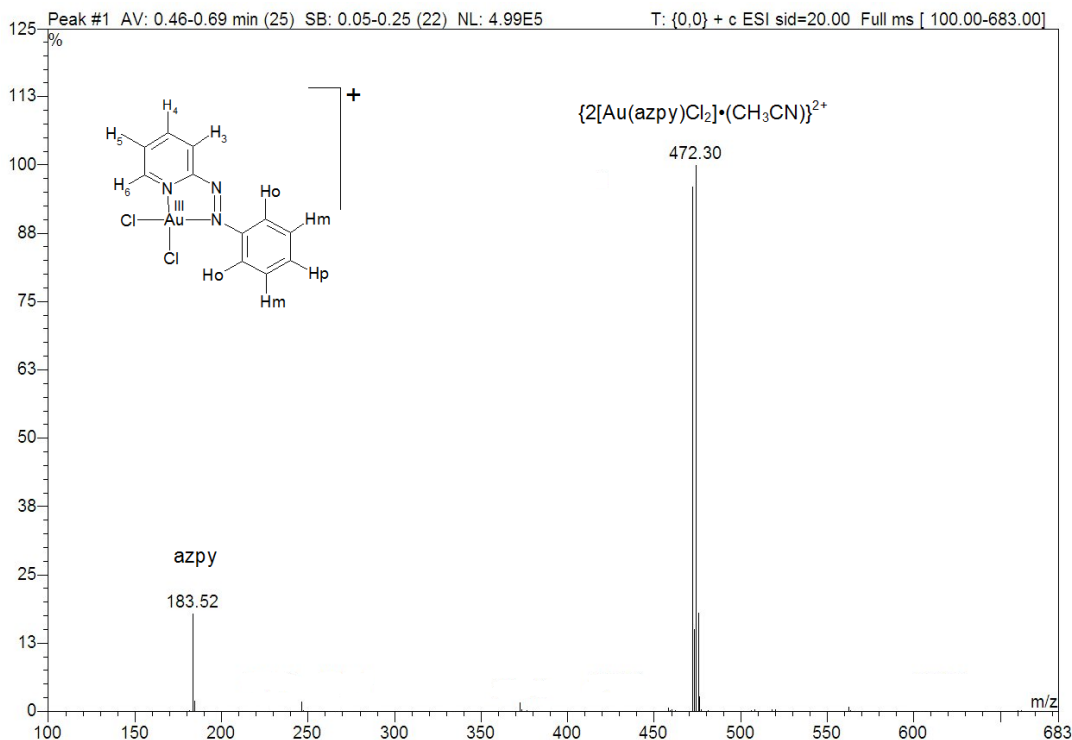


Figure 2.3.9 ESI-MS positive ion spectrum from Au-azpy (m/z in Da).

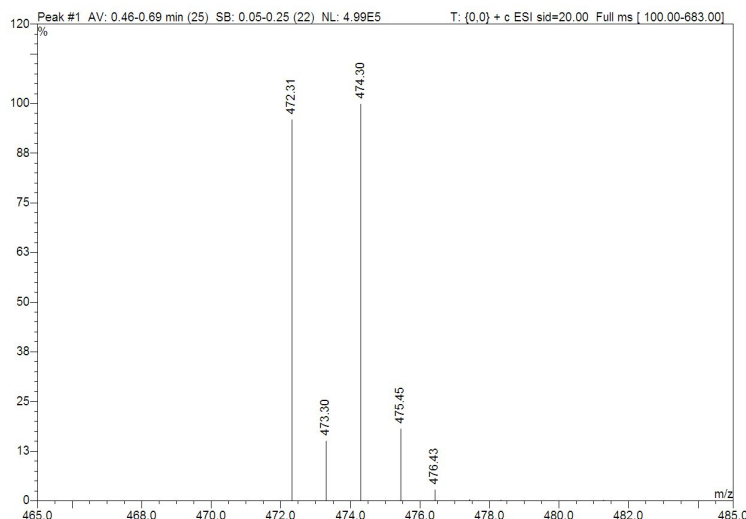


Figure 2.3.10 Expansion of a selected region of the ESI-MS positive ion spectrum from Au-azpy (m/z in Da).

The ESI-mass spectrum of Au-tazpy exhibits a positive peak at $m/z = 465.95$, which corresponds to the cationic structure, $[\text{Au}(\text{tazpy})\text{Cl}_2]^{1+}$. Acetonitrile (CH_3CN) was used as eluent and as in the case of Au-azpy, the peak exhibited the correct isotopomer distribution (spectrum not shown). In case of Au-3mazpy, the ESI-MS spectrum shows three major positive peaks at $m/z=465.66$, 485.81 and 501.14 which correspond to the cationic structures, $[\text{Au}(3\text{mazpy})\text{Cl}_2]^{1+}$, $\{2[\text{Au}(3\text{mazpy})\text{Cl}_2](\text{CH}_3\text{CN})\}^{2+}$ and $\{[\text{Au}(3\text{mazpy})\text{Cl}_2]^{1+}\} \cdot 2\text{H}_2\text{O}$, respectively (spectrum not shown). For Au-4mazpy, the ESI-MS spectrum presents also three major positive peaks at $m/z=500.72$, 483.80 and 465.62, which respectively correspond to the structures, $[\text{Au}(4\text{mazpy})\text{Cl}_2]\text{Cl}$,

Chapter 2

$[\text{Au}(\text{4mazpy})\text{Cl}_2]^{1+}\cdot\text{H}_2\text{O}$ and $[\text{Au}(\text{4mazpy})\text{Cl}_2]^{1+}$ (spectrum not shown). Finally, the ESI-mass spectrum of Au-3mtazpy exhibits three major positive peak at $m/z = 532.86$, 514.72 and 479.65 which corresponds to the structures, $[\text{Au}(\text{4mazpy})\text{Cl}_2]\text{Cl}\cdot\text{H}_2\text{O}$, $[\text{Au}(\text{4mazpy})\text{Cl}_2]\text{Cl}$ and $[\text{Au}(\text{4mazpy})\text{Cl}_2]^{1+}$ respectively. In all the spectra described, all MS peaks exhibited the correct isotopomer distribution mainly derived from the number of chlorine atoms.

The assignments of characteristic IR frequencies for the resulting complexes may be discussed as follows. Assignment of all the peaks was not achieved as IR spectra of the gold(III) complexes are rather complex but some characteristic frequencies in the range $4000\text{--}400\text{ cm}^{-1}$ are observed and the corresponding assignments done. The functional groups C=N, C=C and N=N present in the complexes, develop stretching mode which can be observed in this range. First of all, from IR studies, several changes were observed in the spectrum of the corresponding gold complexes when comparing with the spectrum obtained from the free ligands.

The IR spectra of these complexes show bands in the region $3400\text{--}3150\text{ cm}^{-1}$ which could be assigned to $\nu(\text{O-H})$, from the crystallization water, whereas also sharp bands around 1630 cm^{-1} confirm the presence of crystallization water. The $\nu(\text{C-H})$ vibration of the methyl groups in the organic moiety in the complex (ligands: tazpy, 3mazpy, 4mazpy and 3mtazpy) are detected around $3080\text{--}2900\text{ cm}^{-1}$ (data reported in the experimental section).

Table 2.3.4 summarizes some selected peaks, the corresponding assignment and frequencies in the mid-IR region. All the peaks confirm the presence of the ligand and coordinating to gold.

Table 2.3.4 Selected IR peak assignments for the gold complexes and free ligands.

Compound	Frequencies (cm^{-1})						
	$\nu\text{ C=N}$	$\nu\text{ C=N,}$ $\nu\text{ C=C}$	$\nu\text{ N=N}$	ring breathing mode	$\delta\text{ =N-C=}$	Ring mono substitution	Au-Cl
Azpy	1580-1570s	1490-1430s	1420 vs 1331-1297m	991 m	788-736 vs	684 vs	-
Au-azpy	1616-1592m	1526-1460m	1432m 1358-1300m	1011m	781-720 vs	678 vs	352 vs
Tazpy	1596-1572s	1476-1455s	1414 s 1304-1279m	989 m	788-716 vs	-	-
Au-tazpy	1623-1575m	1520-1475m	1414 m 1339-1281m	1154 m	780-719s	-	352 vs
3mazpy	1573-1560m	1478-1406s	1438 s 1331-1305m	931 w	792-755 vs	686 vs	-
Au-3mazpy	1600-1582	1490-1404m	1455m 1306-1270m	1071 m	790-743 s	684 s	356 vs
4mazpy	1598-1564s	1490-1445m	1446m 1383-1298s	992 m	834-738 vs	684vs	-
Au-4mazpy	1616-1558m	1486-1435m	1486 m 1399 m	1046 m	827-736 s	683 s	358 vs
3mtazpy	1610-1560m	1480-1377s	1453vs 1304-1278m	1041 m	801-712 vs	-	-
Au-3mtazpy	1593-1558w	1478-1436m	1455s 1378w	1134m	771-748 vs	-	357 vs

New bands are observed in the spectra of the complexes at ca 350 cm^{-1} due to the $\nu(\text{Au-Cl})$ vibrations. These are absent in the spectrum of the free ligand. The frequency values are in accordance with a chloride ion in a trans position to the nitrogen of the azo group [40]. For Au-3mazpy, Au-4mazpy and Au-3mtazpy the $\nu(\text{Au-Cl})$ mode is localized at higher frequency most probably due to the presence of the methyl moieties in the pyridyl ring, as more π -electron density is available.

Additional IR evidence of coordination is available. For instance, the azpy ligand showed the N=N stretching vibration at 1420 cm^{-1} , whereas the N=N stretching mode in the complex, Au-azpy, appeared at 1432 cm^{-1} . The increase in frequency in case of the stretching N=N band is suggested to be result of coordination of just one nitrogen from the azo bond, instead of a coordination including both. This change to higher energy indicates less double-bond character in the N=N bond, effect also observed in case of d^8 complexes [41, 42]. It also could prove slight π -bonding to gold through the azo group. The same effect has been observed in all the complexes, although a more dramatic change is observed in Au-3mazpy and Au-4mazpy. The influence of the

methyl moieties in the pyridyl ring probes to be more important than the influence of substituents in the aryl moiety.

Finally, conclusive IR evidence of the coordination of these 2-(arylo)pyridine ligands with the Au(III) is obtained from the C=N and C=C vibration modes. When studying the data for Au-azpy, the changes in the free ligand vibrations are consistent with coordination. The peaks derived from the vibration of the C=N bond are shifted to higher frequency. This shift, in general, is a clear indication of coordination of the pyridine ring to the metal [43]. The ring breathing mode located around 990 cm^{-1} in the free ligand was also shifted to 1011 due to coordination of pyridine. The IR spectrum also exhibits strong absorptions at 1616 , 1459 , 781 , 723 and 678 cm^{-1} which are characteristic of N-bonded pyridine complexes [44]. The shift tendency just described for Au-azpy has also been observed in the other complexes.

The electronic spectra of all the complexes were recorded in freshly prepared acetonitrile solutions, due to the poor solubility in water and the higher stability of the gold compounds in the mentioned solvent. As described earlier, the spectra of the ligands show essentially three bands, two $\pi \rightarrow \pi^*$ -transitions in the range $220\text{--}326\text{ nm}$ with high molar absorption coefficients and one $n \rightarrow \pi^*$ -band around 455 nm with smaller molar absorption coefficients.

The analysis of the changes in the spectra will start with the Au-azpy spectrum (figure 2.3.11). The spectrum is characterized by intense peaks in the region that comprises $200\text{--}550\text{ nm}$. The bands appearing at 225 ($\log \epsilon_M = 4.782$) and 335 ($\log \epsilon_M = 4.386$) are considered mainly as intraligand charge-transfer transitions, as they present high molar absorption coefficients and could be observed in the free ligand [9, 10, 16, 24] as well (figure 2.3.6). In the particular case of the absorption peak at 225 nm a higher LMCT nature is observed due to the extremely high molar absorption coefficient, which is comparable to the one present in the $[\text{AuCl}_4]^-$ anion (230 nm , $\log \epsilon_M = 4.5359$). The energy of the $\pi \rightarrow \pi^*$ -transition in a free azpy (at 315 nm) presents a bathochromic shift in Au-azpy (at 335 nm), which is consistent with coordination of azpy. The transitions involved in a $5d^8$ system are of forbidden g-g nature with molar absorption coefficient values below 100. The typical band for the charge-transfer transition $\text{Cl} \rightarrow \text{Au(III)}$ [45] localized in HAuCl_4 at 315 nm cannot be observed due to overlapping with the other bands. It is not possible either to detect any reduction to Au(I), as the expected absorption at 246 nm [46] is not observed. The molar absorption coefficient for the lowest energy peak is 401 in case of azpy (450 nm) and 741 in case of Au-azpy (440 nm).

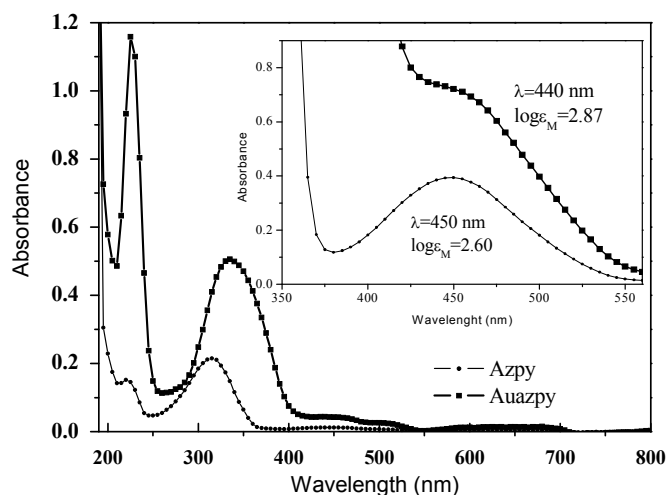


Figure 2.3.11 UV-Vis absorption spectra of azpy and Au-azpy in acetonitrile at 294 K; the inset shows a vertically expanded view of the spectra (higher concentration) in the visible region.

Table 2.3.5 presents the electronic spectral data for the new complexes in CH_3CN at room temperature along with those corresponding to the free ligands. As observed in the Au-azpy spectrum, the high-energy transition (ca 220 nm), which is $\pi \rightarrow \pi^*$ in nature, presents a higher LMCT nature (higher molar absorption coefficient, when compared with the free ligands), which is comparable to the transition present in the $[\text{AuCl}_4]^-$ anion (230 nm , $\log \epsilon_M = 4.5359$). A small blue shift (5 nm) is observed in case of Au3mtazpy (when compared with the free ligand). In case of Au-azpy, Au-tazpy and Au-3mazpy a red shift ($1\text{--}5\text{ nm}$) is observed, while any change is presented in the spectrum of Au-4mazpy.

Chapter 2

More dramatic effects have been observed in the second $\pi \rightarrow \pi^*$ -transition located around 315 nm. For all the new Au(III) complexes a bathochromic shift (12- 24 nm) is observed, which is also consistent with coordination of the ligands. Also worthy to mention is the moderate increase in the molar absorption coefficient, which could also be explained as a result of coordination.

The $n \rightarrow \pi^*$ -transition in the range of 440-484 nm for the gold compounds shows a hypsochromic shift (ca. 10 nm) for Au-azpy and Au-4mazpy and a red shift (8 and 19 nm) in the case of Au-tazpy, Au-3mazpy and Au-3mtazpy. It appears that the presence of the methyl moiety at the *ortho* position with respect to the azo group in the phenyl or tolyl rings produce the dominant effect as the higher shift is observed for Au-3mazpy and Au-3mtazpy. As earlier explained, the presence of metal-to-ligand charge-transfer transitions could not be observed due to the small molar absorption coefficients (ca. 100 for a $5d^8$ system). It was not possible either to detect any impurity of Au(I) species.

Table 2.3.5 Electronic spectral data for the Au(III) complexes and free ligands.

Compound	Wavelength [$\log \epsilon_M$] (nm)		
	$\pi \rightarrow \pi^*$	$\pi \rightarrow \pi^*$	$n \rightarrow \pi^*$
Azpy	220[4.19]	315[4.34]	450[2.60]
Au-azpy	225[4.78]	335[4.39]	440[2.87]
tazpy	- ^a	320[4.20]	454[2.33]
Au-tazpy	227[4.69]	332[4.24]	462[2.95]
3mazpy	224[3.86]	319[3.93]	453[2.66]
Au-3mazpy	225[4.35]	343[4.33]	472[2.70]
4mazpy	225[3.24]	316[3.37]	450[2.58]
Au-4mazpy	225[4.54]	334[4.29]	441[2.70]
3mtazpy	230[3.88]	325[4.10]	465[2.75]
Au-3mtazpy	225[4.46]	347[4.16]	484[2.94]

a: not observed; see text

Gold(III) complexes are diamagnetic ($5d^8$) and display normal ^1H NMR spectra. ^1H NMR spectroscopy also shows clear evidence of coordination and proves to be a useful tool for the characterization of these compounds. The ^1H NMR spectra of all the complexes show resonances due to the protons associated with the ligands. The pyridyl ring *ortho*-protons (H_6) experience a downfield shift in the chemical shift values upon coordination, as compared with the free ligands, while smaller effects on the tolyl and phenyl rings were observed. In all cases the pyridyl protons H_6 , H_5 , H_4 and/or H_3 , when present in the structure, are mutually coupled with each other to yield doublets, triplets and a double doublet. The most downfield signal is ascribed to the *ortho*-proton (H_6), which integrates as one proton.

Figure 2.3.12 shows free *azpy* and *Au-azpy* spectra for comparison reasons, obtained in deuterated acetone. The proton numbering pattern of the complex is also shown. From the ^1H NMR spectrum of *Au-azpy*, seven different peaks accounting for 9 protons are observed; this pattern can be explained by asymmetry in the product formed, which is larger than the asymmetry observed in the free ligand. The integration values are in agreement with the proposed structure (assignment data, 300 MHz, acetone, 294 K, $\delta=9.24620$ (d, 1H, H_6), 9.02453 (t, 1H, H_4), 8.66925 (d, 1H, H_3), 8.38438 (t, 1H, H_5), 8.14607 (m, 2H, H_o) and 7.77802 ppm (m, 3H, 2H_m and H_p)). The very clean spectrum indicates a high purity of the sample. The integral ratio between the peaks also correlates with the chemical structure proposed.

The H_6 doublet in this coordination compound has been assigned on account of its ^3J coupling (typical values of around 5 Hz for the H_6 versus around 9 Hz for the H_3 doublet, as concluded from selective substitution of the pyridine-ring protons) and assignments of the H_4 and H_5 were made on the basis of 2D ^1H COSY experiments (Figure 2.3.13). The broadness in the peak (H_6) is attributed to the presence of the electronegative pyridine nitrogen.

The deshielding effect observed for H_6 is the result of the pyridine nitrogen coordination to the metallic electrophilic centre, as well as the deshielding effect of the chlorides atoms coordinated to gold. As a result of the aromatic resonance in the pyridine ring the coordination

effect could also be the reason for the downfield shift of H₄ located at *para* position with respect to the pyridyl nitrogen.

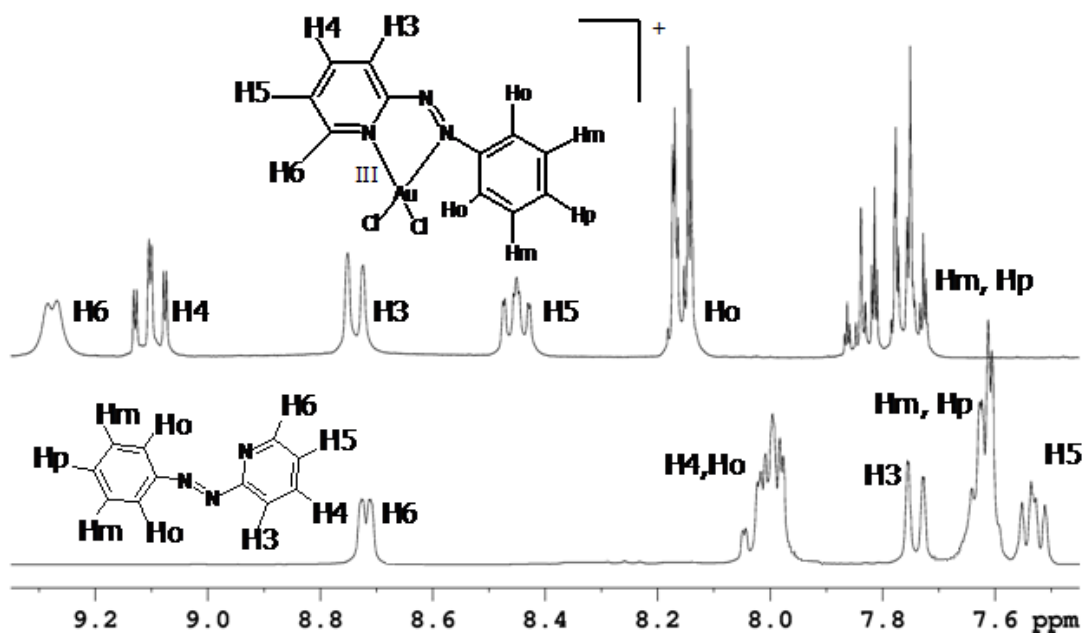


Figure 2.3.12 ^1H NMR spectrum of Au-azpy recorded in deuterated acetone at 294 K, using TMS as internal standard. Aromatic region. The spectrum of free azpy in the same solvent is depicted below for comparison.

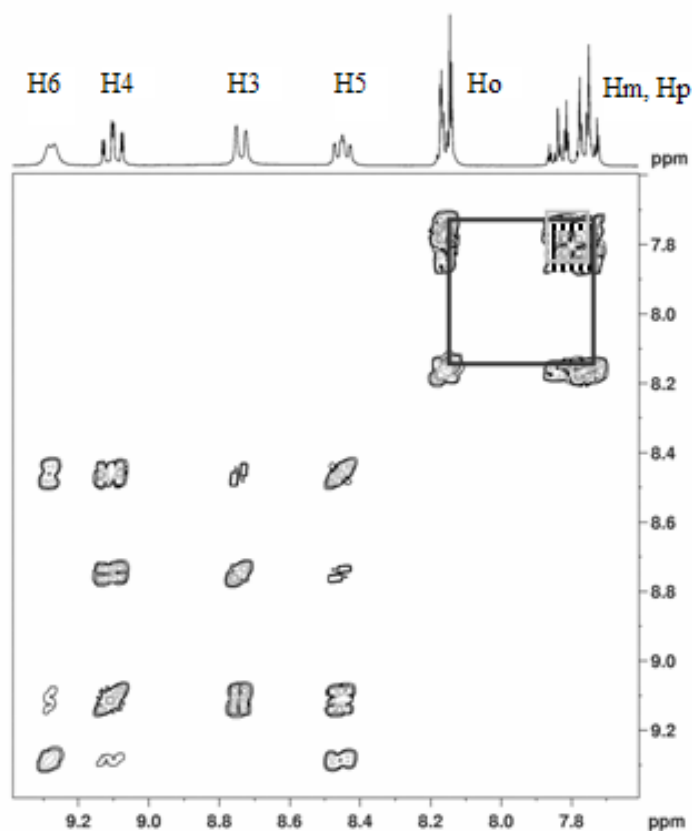


Figure 2.3.13 2D ^1H COSY spectrum of Au-azpy recorded in deuterated acetone at 21 °C, using TMS as internal standard. Aromatic region is shown only.

As expected, the deshielding effect on the aromatic non-pyridine ring is not so strong, but certainly some differences can be observed when comparisons with the starting materials are made. The absence of single peaks for the two H_o and H_m atoms in the spectrum indicates a reduced symmetry for the phenyl moiety, which could be generated by intramolecular interactions e.g. by a Cl–H_o hydrogen bond.

Chapter 2

Similar results were observed in the case Au-tazpy, Au-3mazpy, Au-4mazpy and Au-3mtazpy, where clear evidence of coordination could be pointed out. Figures 2.3.14, 2.3.15, 2.3.16 and 2.3.17 show the spectra of Au-tazpy, Au-3mazpy, Au-4mazpy and Au-3mtazpy respectively with the corresponding free ligands and the numbering pattern in the complexes. The assignment of resonance peaks was based also on the integral ratio between the peaks, shifts and was corroborated by 2D ^1H COSY experiments. All spectra show a high purity of the samples.

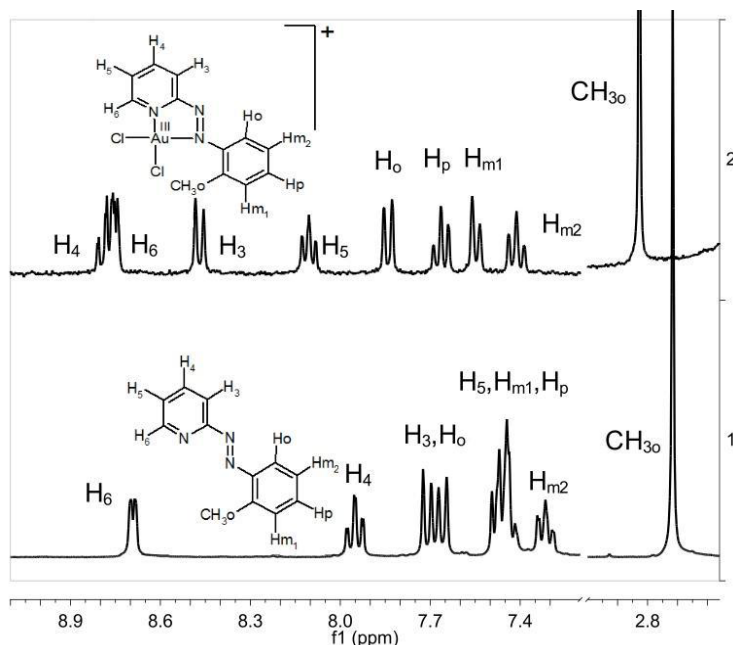


Figure 2.3.14 ^1H NMR spectra of Au-tazpy (2) recorded in deuterated acetonitrile at 21 °C, using TMS as internal standard. The spectrum of free tazpy (1) in the same solvent is also depicted for comparison, as well as the numbering pattern.

In case of Au-tazpy, the coordination of gold produces a small downfield shift for the H_6 proton peak and a bigger effect on H_4 . This effect could be the result of intramolecular interactions. It is clear that coordination affects considerably all protons in the pyridyl ring but also important influence could be detected in the tolyl moiety. The effect of coordination of the azo nitrogen could also be detected in the methyl group located in the tolyl ring.

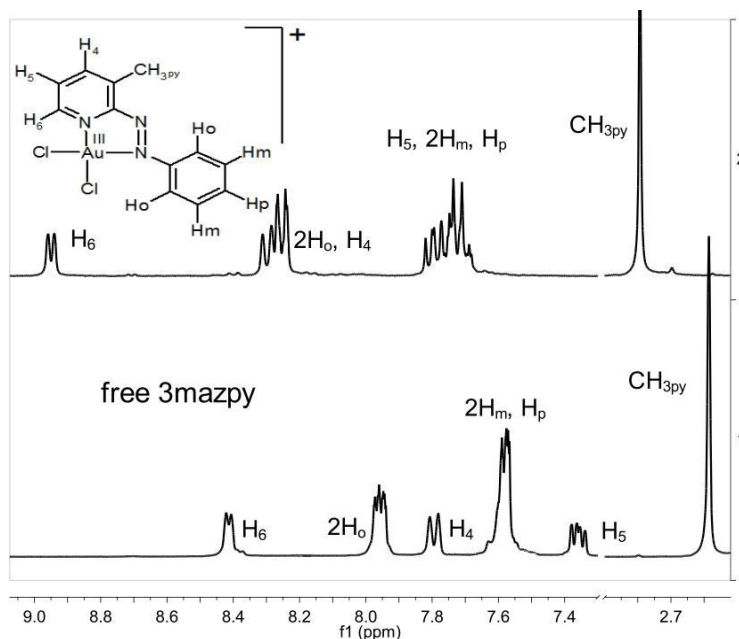


Figure 2.3.15 ^1H NMR spectra of Au-3mazpy (2) recorded in deuterated acetonitrile at 21 °C, using TMS as internal standard. The spectrum of free 3mazpy (1) in the same solvent is also depicted for comparison, as well as the numbering pattern.

Chapter 2

The coordination of gold in Au-3mazpy could be observed from the changes in the spectrum. There is a downfield shift of the H₆ proton peak. H₄ appears to be affected in smaller degree due to the presence of the methyl group, in *ortho* position with respect to it. The H_o protons are magnetically equivalent in solution. The coordination affects considerably all protons in the pyridyl ring, but also important influences have been detected in the phenyl moiety. The methyl group in the pyridyl ring shows a downfield shift, compatible with coordination of this heterocyclic ring.

The spectrum of Au-4mazpy present changes which are compatible with coordination of the ligand to the metal center. There is a downfield shift for the H₆ proton peak. In this compound the effect in the phenyl ring appears to be more pronounced as H_o is localized downfield from the H₃ resonance. The H_o protons are magnetically equivalent in solution. The methyl group in the pyridyl ring shows a downfield shift, compatible with coordination of this heterocyclic ring.

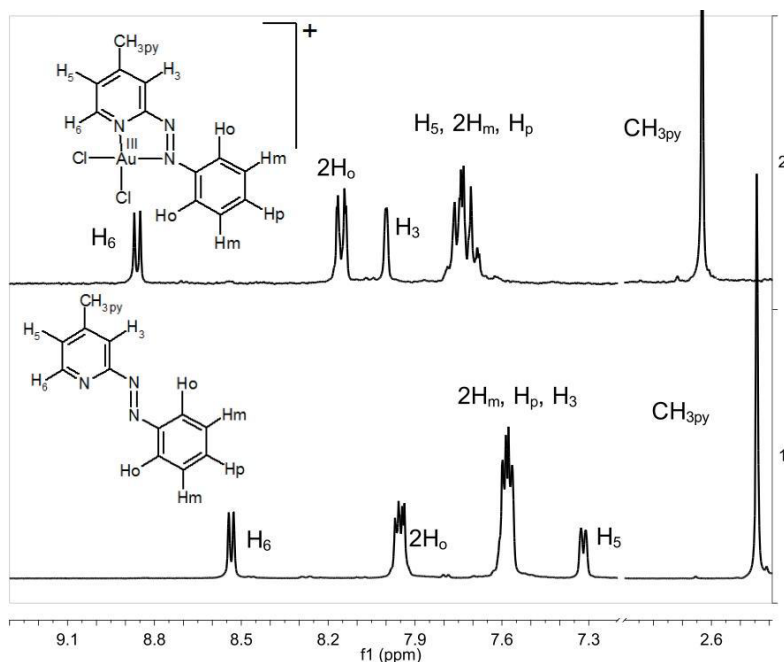


Figure 2.3.16 ¹H NMR spectra of Au-4mazpy (2) recorded in deuterated acetonitrile at 21 °C, using TMS as internal standard. The spectrum of free 4mazpy (1) in the same solvent is also depicted for comparison, as well as the numbering pattern.

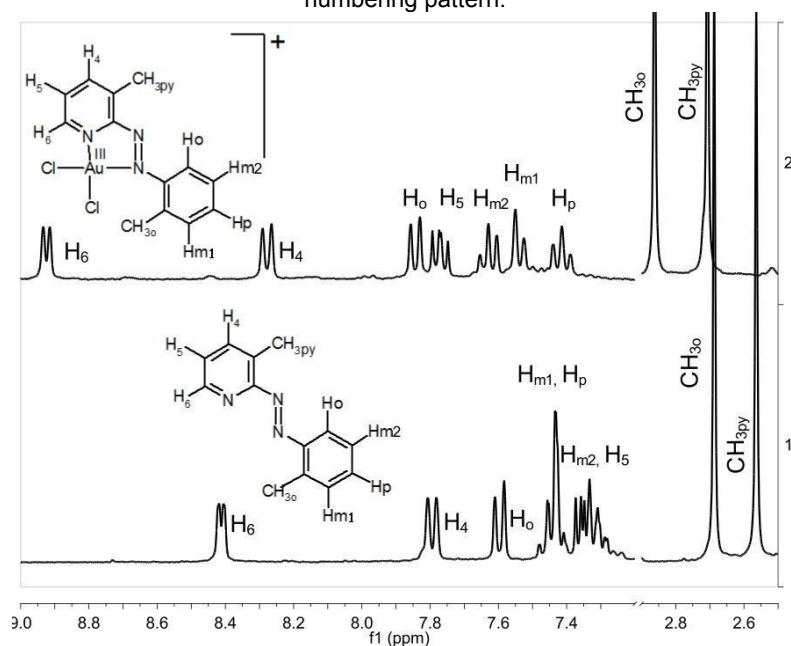


Figure 2.3.17 ¹H NMR spectra of Au-3mtmazpy (2) recorded in deuterated acetonitrile at 294 K, using TMS as internal standard. The spectrum of free 3mtazpy (1) in the same solvent is also depicted for comparison, as well as the numbering pattern.

Finally, the coordination of gold in Au-3tmazpy could be suggested from the changes in the spectrum. There is a downfield shift for the H₆ proton resonance signal. The coordination affects considerably all protons in the pyridyl ring, but also an important influence is visible in the tolyl moiety. The methyl group in the pyridyl ring shows a downfield shift, compatible with coordination of this heterocyclic ring, as well as the downfield shift observed in the methyl group located in the tolyl moiety.

Although the gold(III) complexes described above have not been obtained in the single-crystalline state, and therefore the structure cannot be given in details and in 3D, the conclusions reached upon application of the spectroscopic techniques, strongly suggest that coordination takes place in a near-square-planar geometry through the pyridyl and azo-nitrogen atoms in a bidentate mode and that they lying in the same plane.

2.4. Conclusions

Gold holds a special position among the metals in the periodic table of the elements [47]. For at least three millennia, it has been known as “King of the metals”, or the most noble of the metals referring to its resistance towards most corrosive forces.

Even though the use of gold compounds has been increased in human activities [48], little knowledge has been achieved related to its chemistry. In this context, the study and application of gold(III) compounds as anticancer agents represents a promising field and have attracted attention in the past years owing to the anti-arthritis activity developed by some gold compounds [49-51].

Although gold(III) complexes have demonstrated great potential as antitumor agents, the design of stable complexes has been challenging due to the nature of the gold(III) species. The design of the square planar gold(III) complexes described above was based on two main needs. The first need is the stabilization of gold(III) species, which could be obtained by the coordination of appropriate ligands, in this case, the bidentate nitrogen-donor ligands, 2-(aryloxy)pyridines (the weak σ -donor and strong π -acceptor). The second important design factor is the presence of labile groups which eventually could be able to form strong bonds with biomolecules; for that purpose the new gold(III) complexes described here also contain two labile Au(III)-chloride bonds.

Then, this chapter described the successful synthesis and characterization of a new family of gold(III) compounds with 2-(aryloxy)pyridine ligands. The complexes with general formula, [Au(L)Cl₂]Cl (where L=2-(phenyloxy)pyridine, o-tolyloxy)pyridine, 3-methyl-2-phenyloxy)pyridine, 4-methyl-2-phenyloxy)pyridine and 3-methyl-2-tolyloxy)pyridine), are stable in the solid state and have been fully characterized by means of elemental analysis, IR, UV-Vis, conductivity measurements, ¹H NMR, 2D ¹H COSY studies, ESI-MS and ICP-OES.

The ligands selected for study are derivatized aryloxy)pyridines (with electron-donating groups either in the pyridyl moiety, in the phenyl ring or in both, in an attempt to tune the best stability and biological activity.

This contribution was strongly motivated by the relatively little knowledge that was available of the mechanism of action of gold drugs in particular in the field of cancer treatment.

In the following chapter, the stability of these compounds in solution, as well as the in vitro cytotoxic activity will be described.

2.5. References

- [1] G.J. Higby, *Gold Bull.* 15 (1982) 130-140.
- [2] C.F. Shaw III, *Chem. Rev.* 99 (1999) 2589-2600.
- [3] G.D. Champion, G.G. Graham, J.B. Ziegler, *Baillieres Clin. Rheumatol.* 4 (1990) 491-534.
- [4] S.P. Fricker, *Gold Bull.* 29 (1996) 53-59.
- [5] E.R.T. Tiekink, *Crit. Rev. Oncol./Hematol.* 42 (2002) 225-248.
- [6] E.R.T. Tiekink, *Gold Bull.* 36 (2003) 117-124.
- [7] C. Gabbiani, A. Casini, L. Messori, *Gold Bull.* 40 (2007) 73-81.
- [8] L. Messori, G. Marcon, A. Innocenti, E. Gallori, M. Franchi, P. Orioli, *Bioinorg. Chem. Appl.* 3 (2005) 239-253.
- [9] S. Goswami, A.R. Chakravarty, A. Chakravorty, *Inorg. Chem.* 20 (1981) 2246-2250.
- [10] R.A. Krause, K. Krause, *Inorg. Chem.* 19 (1980) 2600-2603.
- [11] S. Gupta, Chakravorty, *Inorg. Nucl. Chem. Lett.* 9 (1973) 109-112.

Chapter 2

- [12] B.S. Raghavendra, A. Chakravorty, *Indian J. Chem. Sect A-Inorg. Phys. Theor. Anal. Chem.* 14 (1976) 166-169.
- [13] A.K. Ghosh, P. Majumdar, L.R. Falvello, G. Mostafa, S. Goswami, 18 (1999) 5086-5090.
- [14] A.K. Deb, S. Goswami, *J. Chem. Soc.-Dalton Trans.* (1989) 1635-1637.
- [15] P.V. Roling, D.D. Kirt, J.L. Dill, S. Hall, C. Hollstrom, *J. Organomet. Chem.* 116 (1976) 39-53.
- [16] S. Goswami, A.R. Chakravarty, A. Chakravorty, *Inorg. Chem.* 21 (1982) 2737-2742.
- [17] S. Wolfgang, T.C. Streckas, H.D. Gafney, R.A. Krause, K. Krause, *Inorg. Chem.* 23 (1984) 2650-2655.
- [18] R.A. Krause, K. Krause, *Inorg. Chem.* 23 (1984) 2195-2198.
- [19] T. Bao, K. Krause, R.A. Krause, *Inorg. Chem.* 27 (1988) 759-761.
- [20] A.C.G. Hotze, A.H. Velders, F. Ugozzoli, M. Biagini-Cingi, A.M. Manotti-Lanfredi, J.G. Haasnoot, J. Reedijk, *Inorg. Chem.* 39 (2000) 3838-3844.
- [21] R.A. Krause, K. Krause, *Abstr. Pap. Am. Chem. Soc.* 184 (1982) 172.
- [22] A.C.G. Hotze, H. Kooijman, A.L. Spek, J.G. Haasnoot, J. Reedijk, *New J. Chem.* 28 (2004) 565-569.
- [23] A.C.G. Hotze, S.E. Caspers, D. de Vos, H. Kooijman, A.L. Spek, A. Flamigni, M. Bacac, G. Sava, J.G. Haasnoot, J. Reedijk, *J. Biol. Inorg. Chem.* 9 (2004) 354-364.
- [24] A.C.G. Hotze, 'Design of ruthenium anticancer agents. Study of the structure-activity relationships and binding to DNA model bases of ruthenium complexes with 2-phenylazopyridine ligands', PhD Thesis, Leiden University, Leiden, 2003.
- [25] A.H. Velders, 'Ruthenium complexes with heterocyclic nitrogen ligands. Design, synthesis, structural and conformational characterization, biological activity and the binding to DNA model bases', PhD Thesis, Leiden University, Leiden, 2000.
- [26] A. Bharath, B.K. Santra, P. Munshi, G.K. Lahiri, *J. Chem. Soc.-Dalton Trans.* (1998) 2643-2650.
- [27] B.K. Santra, G.K. Lahiri, *J. Chem. Soc.-Dalton Trans.* (1998) 139-145.
- [28] G.K. Lahiri, S. Goswami, L.R. Falvello, A. Chakravorty, *Inorg. Chem.* 26 (1987) 3365-3370.
- [29] R. Roy, P. Chattopadhyay, C. Sinha, S. Chattopadhyay, *Polyhedron* 15 (1996) 3361-3369.
- [30] G.K. Rauth, S. Pal, D. Das, C. Sinha, A.M.Z. Slawin, J.D. Woollins, *Polyhedron* 20 (2001) 363-372.
- [31] A.R. Katritsky, (Ed.). *Advances in Heterocyclic Chemistry* 77 (2001).
- [32] K.C. Kalia, Chakraco.A, *J. Org. Chem.* 35 (1970) 2231-2236.
- [33] S.J. Dougan, M. Melchart, A. Habtemariam, S. Parsons, P.J. Sadler, *Inorg. Chem.* 45 (2006) 10882-10894.
- [34] N. Campbell, A.W. Henderson, D. Taylor, *J. Chem. Soc.* (1953) 1281-1285.
- [35] E.V. Brown, G.R. Granneman, *J. Am. Chem. Soc.* 97 (1975) 621-627.
- [36] L. Sahavisit, K. Hansongnern, Songklanakarinn J. Sci. Technol. 27 (2005) 751-759.
- [37] R.J. Abraham, M. Canton, M. Reid, L. Griffiths, *J. Chem. Soc., Perkin Trans. 2* (2000) 803-812.
- [38] R.J. Abraham, M. Reid, *J. Chem. Soc., Perkin Trans. 2* (2002) 1081-1091.
- [39] W.J. Geary, *Coord. Chem. Rev.* 7 (1971) 81-123.
- [40] J. Vicente, M.T. Chicote, D. Bermudez, *Inorg. Chim. Acta* 63 (1982) 35-39.
- [41] P. Bassignana, C. Cogrossi, *Tetrahedron* 20 (1964) 2361-2371.
- [42] B.S. Raghavendra, R.H. Balundgi, A. Chakravorty, *Indian J. Chem.* 14 (1976) 785-786.
- [43] D.A. Baldwin, A.B.P. Lever, R.V. Parish, *Inorg. Chem.* 8 (1969) 107-115.
- [44] E.C. Constable, T.A. Leese, *J. Organomet. Chem.* 363 (1989) 419-424.
- [45] F.H. Fry, G.A. Hamilton, J. Turkevich, *Inorg. Chem.* 5 (1966) 1943-1946.
- [46] A. Vogler, H. Kunkely, *Coord. Chem. Rev.* 219-221 (2001) 489-507.
- [47] H. Schmidbaur, S. Cronje, B. Djordjevic, O. Schuster, *Chem. Phys* 311 (2005) 151-161.
- [48] H. Schmidbaur, *Gold Bull.* 37 (2004) 136.
- [49] F. Abbate, P. Orioli, B. Bruni, G. Marcon, L. Messori, *Inorg. Chim. Acta* 311 (2000) 1-5.
- [50] S. Carotti, G. Marcon, M. Marussich, T. Mazzei, L. Messori, E. Mini, P. Orioli, *Chem.-Biol. Interact.* 125 (2000) 29-38.
- [51] C.J. O'Connor, E. Sinn, *Inorg. Chem.* 17 (1978) 2067-2071.

Chapter 2
